A Novel Aluminum-Filled Composite Dielectric for Embedded Passive Applications

Jianwen Xu, *Member, IEEE*, Kyoung-Sik Moon, Christopher Tison, and C. P. Wong, *Fellow, IEEE*

***Abstract*—This paper presents the development of a novel aluminum-filled high dielectric constant composite for embedded passive applications. Aluminum is well known as a low-cost and fast self-passivation metal. The self-passivation forms a nanoscale insulating boundary outside of the metallic spheres, which has dramatic effects on the electrical, mechanical, and chemical behaviors of the resulting composites. Influences of aluminum particle size and filler loading on the dielectric properties of composites were studied. Because of the self-passivated insulating oxide layer of fine aluminum spheres, a high loading level of aluminum can be used while the composite materials continues to be insulating. Dielectric property measurement demonstrated that, for composites containing 80 wt% 3.0 μm aluminum, a dielectric constant of 109 and a low dissipation factor of about 0.02 can be achieved. The dielectric constant of epoxy-aluminum composites increased almost 30 times as compared with that of the pure epoxy matrix, which is about 3.5. Die shear tests showed that at such loading level, materials still had good processability and good adhesion toward the substrate. Bulk resistivity measurement, high-resolution transmission electron microscope (HRTEM) observation, and thermogravimetric analysis (TGA) were conducted to characterize the aluminum powders in order to understand the dielectric behavior of aluminum-filled composites. Bimodal aluminum-filled composites were also systematically studied in order to further increase the dielectric constant. Ouchiyama–Tanaka's model was used to calculate the theoretical maximum packing fraction (MPF) of bimodal systems. Based on the calculation, rheology studies were performed to find the optimum bimodal filler volume fraction ratio that led to the best packing efficiency of bimodal fillers. It was found that the viscosity of polymer composites showed a minimum at optimum bimodal filler volume fraction ratio. A high dielectric constant of 160 (@10 kHz) with a low dissipation factor of less than 0.025 was achieved with the optimized bimodal aluminum composites. The developed aluminum composite is a promising candidate material for embedded capacitor applications.**

***Index Terms*—Bimodal composites, capacitors, dielectric material, embedded passives, self-passivation.**

I. Introduction

DISCRETE passive components, such as capacitors, resistors, and inductors, occupy more and more substrate real estate as the active components, such as transistors and integrated circuits (ICs), continue miniaturizing. It is also expected that the numbers of passives will continue increasing in almost all electronic products in the coming decades. Replacing discrete passive components with integral or embedded passives, a new electronic packaging technology in which passive components are integrated inside the substrate, becomes an urgent task for next-generation electronics. Embedded passives offer many advantages. Miniaturization and lower board cost are anticipated since the board area previously occupied by discrete passives is now reduced. Also, with embedded passives, internal parasitic resistance and inductance associated with surface-mounted discrete components can be suppressed. Moreover, due to the elimination of solder joints, embedded passives can also improve the reliability, as solder joint failure is one of the major reasons of electronic system failure. Therefore, embedded passives not only provide increased silicon packaging efficiency and reduced assembly cost, but also improved system performance.

Among all integral passives, embedded capacitors call for special attention due to their wide applications. Currently, surface-mounted discrete capacitors are used in all levels of electronic packaging, including signal decoupling, noise suppression, filtering, tuning, bypassing, termination, and frequency determination. Embedded capacitors are particularly favored by decoupling applications because of their ability to reduce parasitics to an extent beyond the limit of discrete capacitors [1].

Embedded capacitors require development of high dielectric and low cost materials. Ceramic-filled polymer composites have been extensively investigated as candidate materials. Methodology of such approach is to combine the high dielectric constant of ceramic filler and the low processing temperature of polymer matrices such as an epoxy. The highest dielectric constant of ceramic-polymer composite reported is 150 (@10 kHz) by Rao and coworkers [2]; however, the composite requires a very high ceramic filler loading of 85% by volume, or 98% by weight. At such a high filler loading, the composite has poor adhesion to substrate and other poor mechanical properties as well; moreover, uniform dispersion of ceramic filler within the epoxy matrix can hardly be achieved. To solve this problem, extensive attention has been focused on insulator–conductor composites near the percolation threshold [3]–[6]. Pecharroman and Moya [6] experimentally observed an ultrahigh dielectric constant of 500 000 in molybdenum-filled ceramic–metal composites (cermets). Rao *et al.* [7] demonstrated that epoxy–silver composite materials have high dielectric constant (> 1000) and high reliability performance suitable for embedded passive application. In the percolative epoxy–silver composite, a low filler loading close to but not exceeding the percolation threshold is used to obtain a high dielectric constant, whereas for polymer-ceramic composites, a high filler loading is used because a higher filler loading will generally lead to a higher dielectric constant. Because the material processibility and adhesion strength deteriorate when the filler loading increases, the lower filler loading

Manuscript received Jul 20, 2003; revised May 25, 2005 and January 5, 2005. This work was supported in part by the National Science Foundation.

The authors are with the School of Materials Science and Engineering, Packaging Research Center, Georgia Institute of Technology, Atlanta, GA 30332 USA (e-mail: cp.wong@mse.gatech.edu).

Digital Object Identifier 10.1109/TADVP.2006.874701

1521-3323/$20.00 © 2006 IEEE

Authorized licensed use limited to: IEEE Xplore. Downloaded on October 7, 2008 at 8:41 from IEEE Xplore. Restrictions apply.

used in the percolative epoxy–silver composites leads to a better material processibility and adhesion strength when compared to the epoxy–ceramic composites. However, a percolative composite requires a precise control of filler loading (to $\pm 0.1\%$ by volume) and extreme uniform distribution of filler. Practically, it's impossible to fulfill such demanding uniform distribution over a large area at all. Moreover, silver is an expensive metal, which will increase the cost of final products.

Because the composition window of a high dielectric constant epoxy–silver composite is too narrow for industry manufacturing, to achieve a wider composition window, we have developed a novel low-cost aluminum-filled high dielectric constant composite. Aluminum is well known as a fast self-passivation and low-cost metal. The thin passivation layer forms an insulating boundary layer outside of the metallic spheres, which has dramatic effects on the electrical, mechanical, and chemical behaviors of the resulting composites. Influences of aluminum particle size and filler loading on the dielectric properties of composites were studied. Due to the self-passivated insulating oxide of fine aluminum spheres, high loading level of aluminum can be used while the composite materials continued to be insulating. Dielectric property measurements demonstrated that, for composites containing 80 wt% 3.0 μm aluminum, a dielectric constant of 109 and a low dissipation factor of about 0.02 (@10 kHz) can be achieved. At such loading level, materials showed good processability and good adhesion to the substrate. Bulk resistivity measurement, high-resolution transmission electron microscope (HRTEM) observation, and thermogravimetric analysis (TGA) were conducted to characterize the aluminum powders, in order to understand the dielectric behavior of aluminum-filled composites. To further increase the dielectric constant, bimodal aluminum-filled composites were also systematically studied. Ouchiyama–Tanaka's model was used to calculate the theoretical maximum packing fraction (MPF) of bimodal systems. Based on the calculation, rheology studies were performed to find the optimum bimodal filler volume fraction ratio that led to the best packing efficiency of bimodal fillers. It was found that the viscosity of polymer composites showed a minimum at optimum bimodal filler volume fraction ratio. A high dielectric constant of 160 (@10 kHz) with a low dissipation factor of less than 0.025 was achieved with the optimized bimodal aluminum composites.

II. Experimental

A. Material Preparation

Epoxy resin was chosen as the polymer matrix because of its ease of processing and its good compatibility with printed wiring board (PWB) manufacturing. The bisphenol-A type resin Epon828 was from Shell Chemicals Company. MHHPA (methylhexahydrophthalic anhydride), from Lindau Chemicals, Inc., and 2E4MZ-CN (1-cyanoethyle-2-ethyl-4-methylimidazole), from Shikoku, Ltd., were used as the hardener and curing catalyst, respectively. The equivalent ratio of epoxide to anhydride was set to be 1:0.85. A cured bisphenol-A epoxy has a dielectric constant of about 3.5 and a dielectric loss of about 0.015. Three spherical aluminum powders were used. The average particle sizes were about 10.0 μm, 3.0 μm, and 100 nm, respectively. The aluminum oxide powder, with average particle size of about 42 nm, was supplied from Nanophase Technologies Corporation.

The 2E4MZ-CN was first dissolved in the MHHPA and then the Epon828 was added into the solution. The epoxy system was carefully mixed in a centrifugal machine (from Glas-Col Company) for two hours. To achieve uniform distribution of metal powders inside the epoxy system, a three-step mixing procedure were taken. First, the composites were hand-stirred for 15 min as a premixing step. Second, the paste from the first step is further dispersed in an ultrasonic chamber (Model 75HT, from VWR Scientific Products) for 30 min. Finally, a high shear blender (from Eberbach Corporation) was used in order to break down the agglomeration of fine filler powders.

B. Capacitor Fabrication and Dielectric Measurement

Glass slides served as the bottom electrode of capacitors after being deposited with a thin layer of titanium and copper by a dc sputterer (from CVC Products Corporation). The composite material was coated onto the slide with a bar coating method. Next, the whole sample was cured with an optimized step-curing procedure in an oven. Finally, the dc sputterer deposited another layer of copper onto the material through a mask, to serve as top electrodes. Dielectric measurement was conducted with an HP 4263A LCR meter, at the frequencies of 10 kHz to 10 MHz. And an RF impedance and dielectric analyzer (Agilent, model E4991A) was used for the characterization of the frequency responses of dielectric properties up to the gigahertz range ($\leq$ 1.5 GHz). For RF impedance and dielectric analyzer measurement, the sample preparation method was different from the above mentioned method; there was no need of dc sputtering for electrodes, and the samples used were thicker than those measured by the LCR meter.

Dielectric constant was calculated from the measured capacitance data, according to the following equation:

$$C = \frac{\varepsilon_0 \varepsilon_r A}{t} \tag{1}$$

where ε_0 is the permittivity of the free space (8.854×10^{-12} F/m), A is the area of capacitor electrode, and t is the thickness of dielectric layer. ε_r is the dielectric constant of measured composite material.

C. DSC Measurement

The curing profile of bisphenol-A epoxy system was studied by a modulated differential scanning calorimeter (DSC, Model 2920, from TA Instruments). Based on the curing profile of bisphenol-A epoxy system, as shown in Fig. 1, three different step-curing profiles were investigated in order to determine the best curing procedure for aluminum filled composites. Three curing profiles were as follows: 1) 120 °C for 15 min, then 140 °C for 1 h; 2) 120 °C for 15 min, then 145 °C for 1 h; 3) 120 °C for 15 min, then 150 °C for 1 h. All dynamic scans were performed at heating rate of 5 °C/ $\min$ under N_2 purge.

The curing procedure was optimized based on three criteria. First, it should have a soft baking step to evaporate the solvent, because at high aluminum loading level, solvent must be used

Authorized licensed use limited to: IEEE Xplore. Downloaded on October 7, 2008 at 8:41 from IEEE Xplore. Restrictions apply.

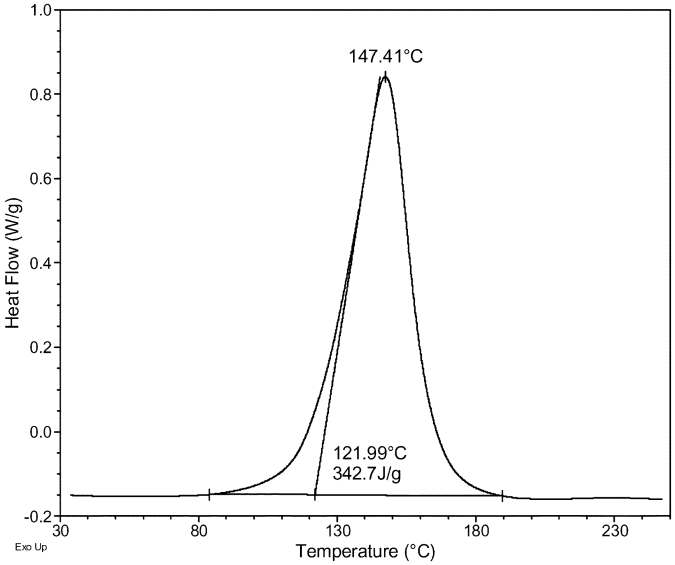

Fig. 1. Curing profile of a bisphenol-A epoxy system.

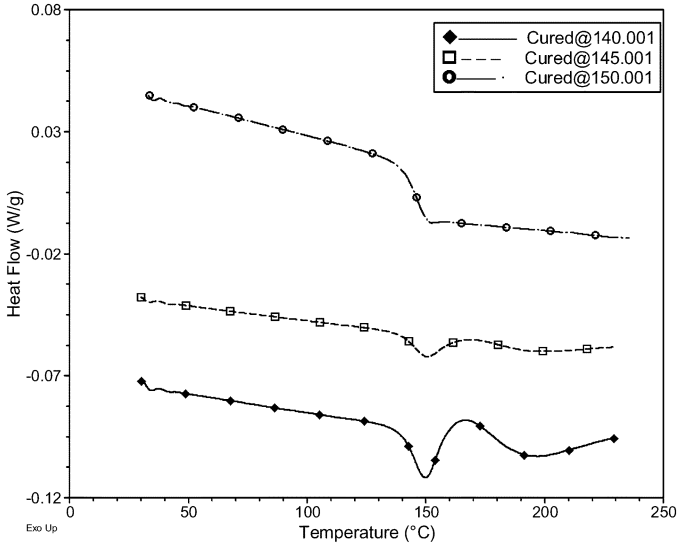

Fig. 2. Heat flow as a function of temperature of 60 wt% aluminum filled composites cured under three different step-curing profiles: 1) 120 °C for 15 min, then 140 °C for 1 h; 2) 120 °C for 15 min, then 145 °C for 1 h; 3) 120 °C for 15 min, then 150 °C for 1 h.

in order to achieve good dispersion of aluminum particle into the matrix. According to the curing profile of the epoxy system, shown in Fig. 1, the onset temperature of curing was around 122 °C. Therefore, 120 °C was selected to be the soft baking temperature, in that the curing process of epoxy is very slow at this temperature; thus the solvent has enough time to vaporize without voiding. Second, the final curing temperature should be high enough to guarantee complete curing of epoxy; otherwise, the uncured part will cause the properties of the ultimate composite to change gradually in the long run of service. Third, the curing temperature should not be too high, since high curing temperature not only leads to evaporation of hardener HMPA, whose boiling point is less than 150 °C, but also causes the precipitation of filler particle as the viscosity decrease with the increase of curing temperature. High curing temperature also induces thermomechanical stresses on the PWB substrate. The peak curing temperature of the epoxy system is 147 °C; based on this, three final curing temperatures, 140 °C, 145 °C, and 150 °C were investigated.

Fig. 2 showed the heat flow as a function of temperature of 60 wt% aluminum-filled composites cured under three different step-curing profiles. Nonreversible heat flow as a function of temperature is given in Fig. 3. Under curing temperatures 140 °C and 145 °C, the aluminum-filled composites were not completely cured. Their curing degrees were 98.4% at 140 °C, and 99.5% at 145 °C, respectively. However, the curing of aluminum composites was complete under a curing temperature of 150 °C, which was then chosen as the curing temperature of aluminum composites.

D. Microscope Observation

A JOEL 4000EX HRTEM, operating at 400 kV, was used to analyze the particle size of aluminum powder and the thickness of its oxide layer. Morphologies of aluminum-filled composites were observed by an optical microscopy (Type 020-520-007 DMLP, Leico Microsystems, Germany). Crossection of samples was polished with grinding papers before observation.

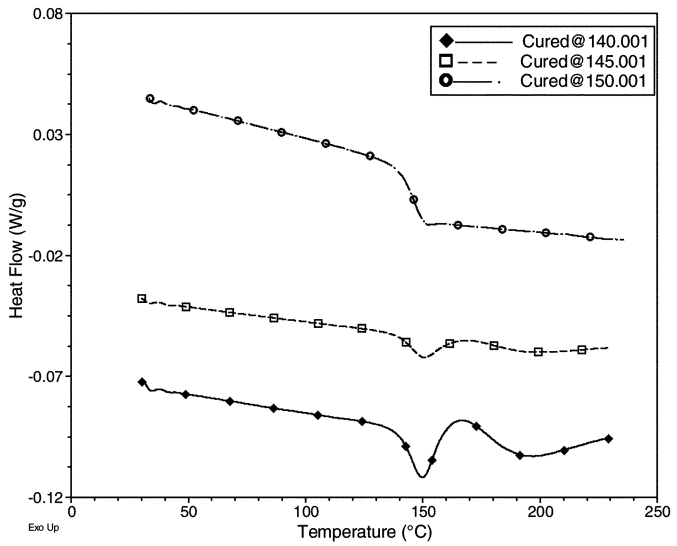

Fig. 3. Nonreversible heat flow as a function of temperature of 60 wt% aluminum filled composites cured under three different step-curing profiles: 1) 120 °C for 15 min, then 140 °C for 1 h; 2) 120 °C for 15 min, then 145 °C for 1 h; 3) 120 °C for 15 min, then 150 °C for 1 h.

E. Rheology Studies

Viscosity of aluminum-filled composites was investigated by a stress rheometer (Model AR1000-N, from TA Instruments). The experiments were performed under steady-state flow procedure with parallel-plate geometry at 25 °C.

F. Bulk Resistivity Measurement

Bulk resistivity of aluminum powder was measured by an in-house made device, using a polymethyl methacrylate (PMMA) pipe with metal electrodes placed on each end after it had been filled with sample powder. Load was applied on the electrodes by a hydraulic unit (from Carver, Inc.). Resistance of the powder under selected load was then measured by a multimeter (from Keithley, Inc.).

Authorized licensed use limited to: IEEE Xplore. Downloaded on October 7, 2008 at 8:41 from IEEE Xplore. Restrictions apply.

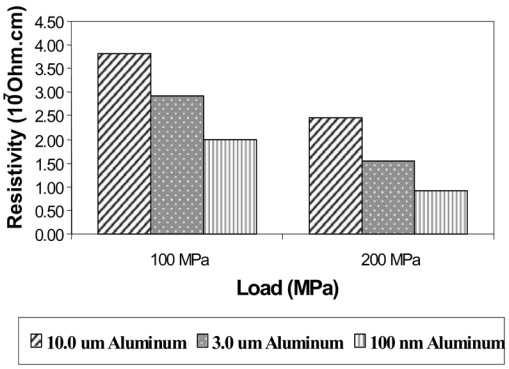

Fig. 4. Bulk resistivity of aluminum powders.

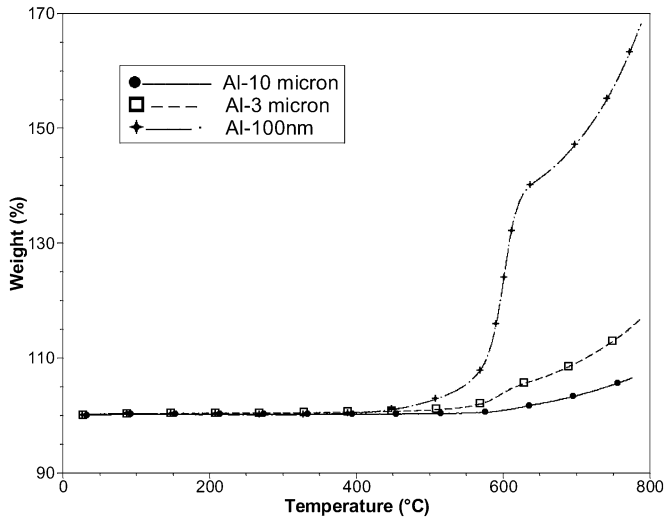

Fig. 5. TGA analysis of aluminum powder.

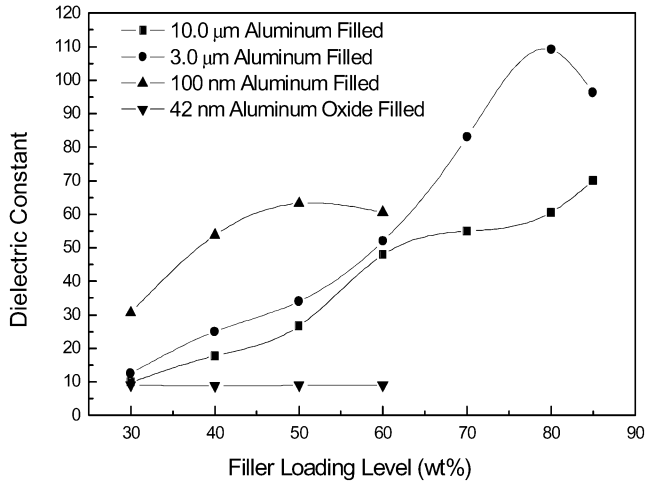

Fig. 6. Dielectric constant of aluminum filled composites as a function of filler loading (@ 10 kHz).

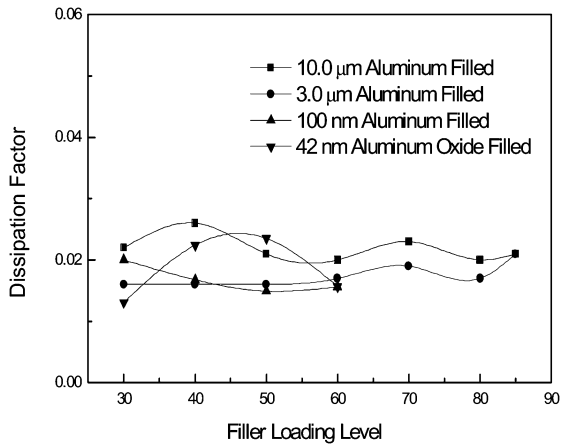

Fig. 7. Dissipation factor of aluminum-filled composites as a function of filler loading (@ 10 kHz).

G. TGA

Thermogravimetric analysis was conducted with a TGA from TA Instruments (Model 2050). The heating rate was 10 °C/min. Air was used as the purge environment.

H. Die Shear Measurement

Adhesion strength of the aluminum composites toward Cu surface was characterized by the die shear measurement. Copper-laminated FR-4 board was cut into both small (4×4 mm) and large (20×20 mm) dies. The dies were cleaned in isopropyl alcohol in an ultrasonic chamber for 5 min, and then rinsed with water. Glass beads (0.5 wt%, diameter 75 μm) were used as spacers to control the distance between upper and lower dies. The small die was placed onto a thin film of composite material to form a layer of tested material, and then put onto the large die. Die shear tests were performed on a bond tester (Model 550-100K, Rouce Instruments), with a blade speed of 100μm/sec.

III. Results and Discussion

Aluminum is a type of instantaneous self-passivation metal when exposed to the oxygen source. The thin passivation oxide layer forms a nanoscale insulating boundary layer outside of the metallic spheres, which has dramatic effects on the electrical, mechanical, and chemical behaviors of the resulting composites. As shown in Fig. 4, bulk resistivities of all three aluminum powders are in the magnitude of 10^7 ohm.cm, which corresponds to semiconducting materials, completely different from electrically conductive aluminum metal.

After instant surface passivation when exposed in the ambient condition, aluminum particles become very stable, as can be seen from thermogravimetric analysis in Fig. 5. The weight gain of aluminum from 25 °C to 400 °C is only about 0.07% for 3.0-μm and 10.0-μm aluminum powders, and about 0.30% for nanoaluminum powder. As temperature further increases, the weight gain of aluminum powders increases dramatically due to the damage of protective aluminum oxide layer.

Figs. 6 and 7 show the dielectric constant and dissipation factor of aluminum-filled composites, respectively. The 3.0-μm and 10.0-μm aluminum can be easily loaded up to 85 wt% in bisphenol-A epoxy. However, for 100-nm nanoaluminum filler, it's difficult to uniformly disperse aluminum particles when filler loading is higher than 50 wt%, as is for 42-nm nanoaluminum oxide filler. The dielectric constant of aluminum filled composites increases with the filler loading level, except at very high filler loading level, e.g., 10.0-μm aluminum

Authorized licensed use limited to: IEEE Xplore. Downloaded on October 7, 2008 at 8:41 from IEEE Xplore. Restrictions apply.

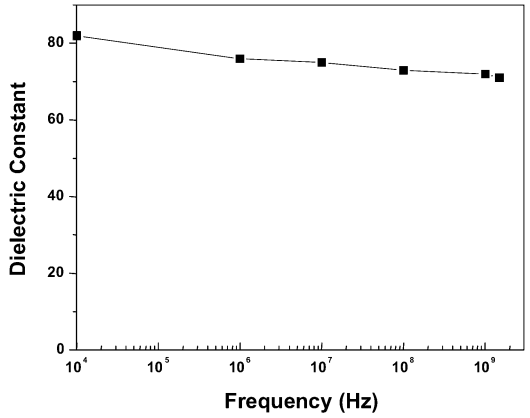

Fig. 8. Frequency dependence of aluminum-filled composites.

composites show a lower dielectric constant at 85 wt% than at 80 wt%. This probably is due to voiding (porosity) from imperfect filler packing at high filler loading levels as well as solvent evaporation because a large amount of solvent is required to disperse filler at such a high filler loading. The 3.0-μm aluminum composites have a higher dielectric constant than that of the 10.0-μm aluminum composites, and the maximum dielectric constant values achieved are 109 for the former and 70 for the latter, which are about 30 and 20 times higher than that of a neat epoxy (about 3.5), respectively. At the same filler loading, 100-nm nanoaluminum composites have a higher dielectric constant than the other two kinds of aluminum composites. The highest dielectric constant is 60 at 50 wt% for nanoaluminum composites. As compared with nanoaluminum oxide-filled composites, the dielectric constant of aluminum-filled composites is much higher, which indicates the metal core inside the self-passivated aluminum oxide layer plays an important role in determining the dielectric constant of aluminum composites. All composites studied here, including aluminum composites and aluminum oxide composites, show very low dissipation factor, i.e., around 0.02, which is desirable for embedded passive applications.

Frequency dependence of 70 wt% 3 μm aluminum-filled composites is shown in Fig. 8. The dielectric constant of aluminum-filled composites is stable in terms of frequencies, and there is only a slight decrease of the dielectric constant when the test frequency increases from 10 kHz to 1.5 GHz. Such a frequency-independent behavior is consistent with the dielectric behavior of polymer–ceramic composites [2] as well as ceramic/metal (cermets) percolative composites [6].

The high dielectric constant of aluminum composites can be explained by the percolation behavior of insulator–conductor composites, even though the aluminum particles were measured to be semiconducting because of an insulating self-passivated oxide layer coated on the aluminum metallic core. For a typical insulator–metal composite system, the electric and dielectric properties near percolation threshold can be predicted by the percolation theory. According to the percolation theory, the properties of physical quantities such as the dc electrical conductivity and effective dielectric constant of a percolation system should exhibit a power-law behavior. The effective dielectric constant (ε) can be described by the following equation [3]–[6]:

$$\varepsilon = \frac{\varepsilon_D}{|f_c - f|^q} \tag{2}$$

where ε_D is the dielectric constant of dielectric phase (or dielectric matrix), q is the scaling constant, f is the percentage of the conductor, and f_c is the percolation threshold at which the conductivity of insulator–conductor composite increases dramatically when f approaches f_c from below the percolation threshold. In the above equation, the effective dielectric constant of a percolative composite is proportional to the dielectric constant of the insulator, which indicates the insulator is the "true" dielectric material, whereas the metal particles in the percolative composites can greatly reduce the effective dielectric thickness. The insulator–conductive filler composite could be considered as a super capacitor network, with a very large electrode area and small dielectric thickness, because each metal particle can act as an electrode of each tiny capacitor in the composite. Therefore, the effective dielectric constant of the insulator–conductive filler composite could be three or four orders of magnitude higher than the dielectric constant of the insulating matrix when the filler loading is close to the percolation threshold [6].

Because of the self-passivated insulating oxide layer on the aluminum particle surface, the epoxy–aluminum composites continued to be insulating even at high filler loading levels. However, the existence of aluminum metallic core can still dramatically reduce the effective dielectric thickness. However, different from a typical percolation system, the dielectric layers, i.e., the thin layers of insulator between the metal cores, include two materials, i.e., the epoxy matrix and the unique nanoscale self-passivated insulating aluminum oxide. Because the dielectric layers are very thin and become thinner as a greater fraction of metallic spheres have been added in, a large capacitance can be observed in the aluminum composites. Since the pure nanoaluminum oxide filler has no such metallic core as in an aluminum particle, the nanoaluminum oxide-filled composites do not show any percolation-related behavior and a much lower dielectric constant was observed, as can be seen in Fig. 6. A unique characteristic of epoxy–aluminum composites is that the self-passivated insulating oxide layer of an aluminum particle is very uniform and dense and thereby can effectively control the dielectric loss of the epoxy–aluminum composites. As such, a low dissipation factor comparable to that of a neat epoxy is observed in the composites, because the epoxy matrix is the "true" dielectric material in the composites.

To further understand the relationship between the aluminum particle size and dielectric behavior of aluminum composites, a 400-kV JOEL HRTEM was used to characterize the aluminum particles. Fig. 9 shows the micrograph of 100-nm aluminum powder from the HRTEM observation. Fig. 10 shows the HRTEM micrograph of a single 100-nm aluminum particle. The dark area in the center is the aluminum metallic core, and the light-grey layer surrounding the metallic core is the self-passivated insulating aluminum oxide. The insulating oxide layer is very dense and uniform. An oxide thickness of 2.8 nm was observed for the 100-nm aluminum powder used in this work. And the self-passivated oxide thickness is about

Authorized licensed use limited to: IEEE Xplore. Downloaded on October 7, 2008 at 8:41 from IEEE Xplore. Restrictions apply.

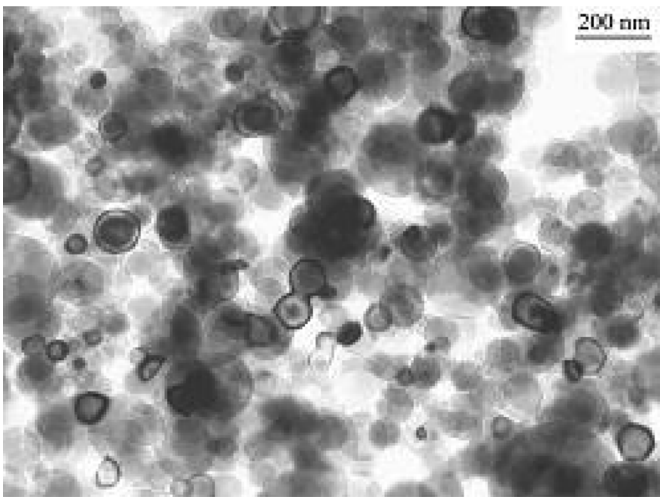

Fig. 9. HRTEM micrograph of 100-nm aluminum powder (400 kV).

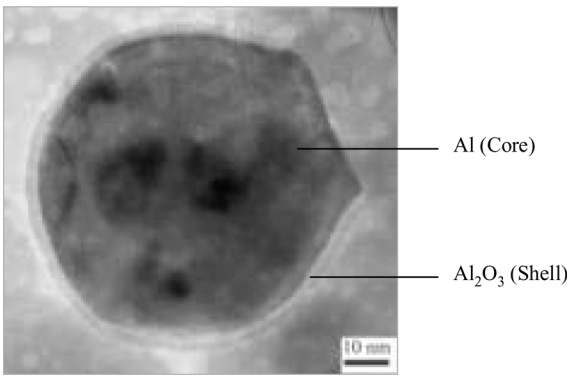

Fig. 10. HRTEM micrograph of a single 100-nm aluminum particle (400 kV).

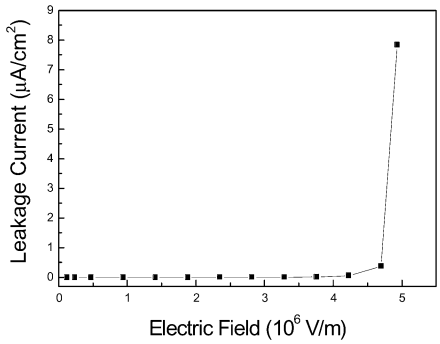

Fig. 11. Leakage current of aluminum-filled composites as a function of electric field.

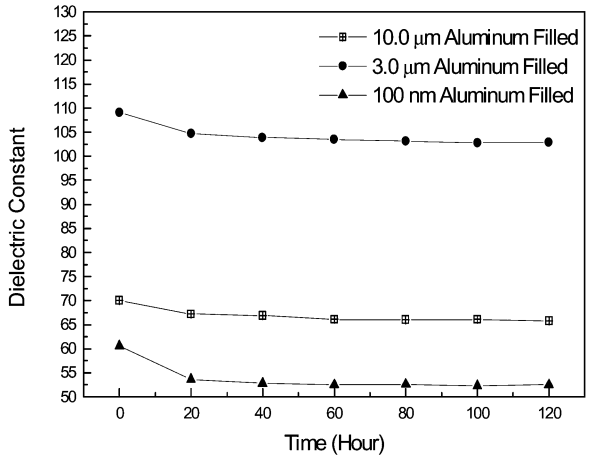

Fig. 12. Influence of 85 °C/85% relative humidity aging on the dielectric constant of aluminum-filled composites.

1 nm for a 10-nm aluminum particle. For bulk aluminum, the thickness of self-passivated insulating oxide is 4–5 nm at room temperature [8]. Therefore, the thickness of oxide layer is dependent on the aluminum particle size and it becomes thinner as the aluminum particle size decreases. The thinner insulating oxide thickness makes the smaller aluminum particle more conductive, which agrees well with the experimental data in bulk resistivity measurement, as shown in Fig. 4. The thickness of the aluminum particles also plays an important role in determining the dielectric behavior of epoxy–aluminum composites. At the same filler loading, the epoxy–aluminum composites filled with smaller particles show a higher effective dielectric constant than with the bigger particles, because the thinner oxide layer of a smaller aluminum particle may make its composites closer to a typical insulator–metal percolative composite without self-passivated insulating oxide on the metal core.

Fig. 11 shows the leakage current versus electric field of 70 wt% 3.0 μm aluminum-filled composite. Leakage current is low and increases slightly when the electric field is below 4.7 MV/m, but increases quickly when voltage further increases. The breakdown field of aluminum composites is much lower than that of polymer–ceramic composites, which is at least above 10 MV/m [2].

Fig. 12 shows the dielectric constant of aluminum-filled composites as a function of 85 °C/85% relative humidity aging time. Samples used were 80 wt% 3.0 μm aluminum-filled composite, 80 wt% 10.0 μm aluminum-filled composite, and 50 wt% nanoaluminum-filled composite. For all samples, the dielectric constant decreases with the aging time in the first 20 h. After that, the dielectric constant exhibits almost no change with time. Smaller particle filler leads to a greater change in dielectric constant of composite materials than does larger particle filler. The change of dielectric constant is related to moisture absorption. Fig. 13 shows the weight gain of aluminum composites during 85/85 aging. Moisture absorption is evident in the first 20 h, as the weight gain is around 1.7 wt% during this period; however, there is almost no difference in weight gain between different-sized aluminum-filled composites. Further oxidation of aluminum filler may account for the difference in dielectric constant change of different-sized aluminum-filled composites. Smaller particles are more active, as found in TGA analysis; therefore, they are more readily further oxidized in 85/85 thermal humidity conditions. Larger particles have less further-oxidation during aging; therefore, less change of dielectric constant was found.

Mechanical properties such as the adhesion strength of a dielectric material to the substrate are important parameters for embedded capacitor applications. In this paper, adhesion strength of the aluminum composites toward Cu surface was characterized by the die shear measurement. Fig. 14 shows die shear strength of 3.0-μm aluminum-filled composites, 10.0-μm

Authorized licensed use limited to: IEEE Xplore. Downloaded on October 7, 2008 at 8:41 from IEEE Xplore. Restrictions apply.

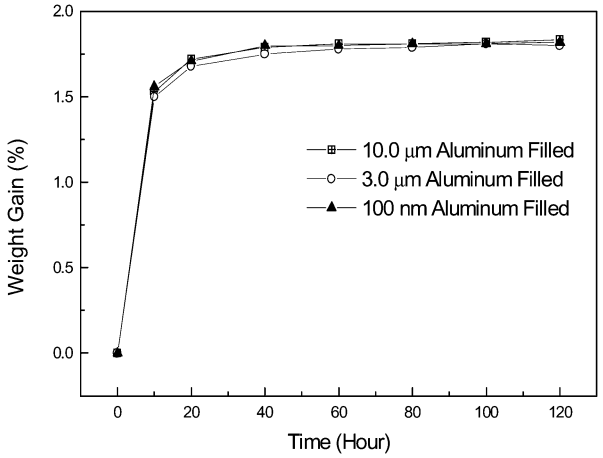

Fig. 13. Weight gain of aluminum composites during 85 °C/85% relative humidity aging.

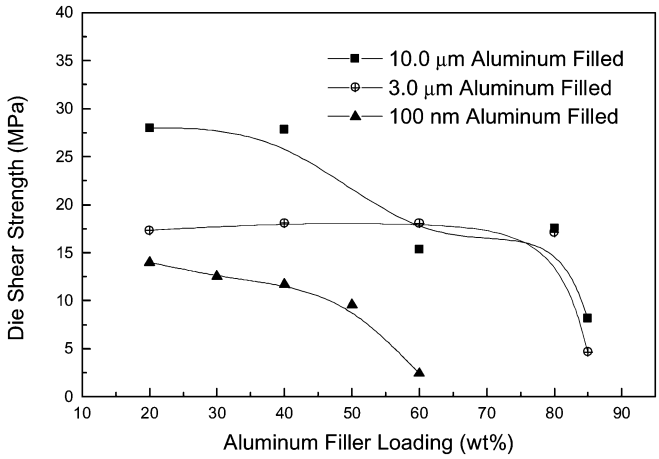

Fig. 14. Die shear strength of aluminum-filled composites.

aluminum-filled composites, and nanoaluminum-filled composites. The die shear strength decreases with the increase of filler loading as the amount of epoxy resin is reduced. Particularly, there is a dramatic decrease when the loading increases from 80 wt% to 85 wt% for 3.0 μm aluminum-filled composites and 10.0 μm aluminum-filled composites, and from 50 wt% to 60 wt% for nanoaluminum-filled composites. In aluminum-filled composites, epoxy resin serves as the adhesive binding the filler together. At high filler loading level, there is not enough epoxy to bind the filler, which results in the dramatic decrease of adhesion strength. However, at 80 wt% aluminum filler loading, the die shear strength is still 17.13 and 17.58 MPa for 3.0-μm aluminum and 10.0-μm aluminum, respectively, which indicates the aluminum filled composites will have good adhesion to the copper layer when incorporated into the substrate structure.

From Fig. 6, it was found that the dielectric constant of an aluminum-filled composite increases with the filler loading level, except at high filler loading levels where voiding (porosity) may occur due to the imperfect packing of filler particles or the solvent evaporation. To achieve the highest dielectric constant for aluminum-filled composites, the packing efficiency in the composites should be maximized in order to reduce the porosity. The filler packing efficiency of a given system is related to the viscosity of entire system. The viscosity of composites controls the dispersibility of filler in the system. It's well known that polydispersity of filler size can reduce the viscosity of a filled system, in particular, at high filler loading level the viscosity can be dramatically reduced by the increased particle size modality. Poslinski [9] found that a minimum viscosity of the composites could be achieved when the bimodal filler ratio is near the theoretical maximum packing fraction (MPF), which in turn indicates higher filler loading can be used with such bimodal combination for the composites.

TABLE I
THEORETICAL MAXIMUM PACKING FRACTIONS OF BIMODAL SYSTEMS

Filler Combination		MPF	Volume fraction of Large Particle	Volume fraction of Small Particle
Large Particle	Small Particle			
10.0 μm	3.0 μm	0.735	0.75-0.82	0.25-0.18
10.0 μm	100 nm	0.891	0.76	0.24
3.0 μm	100 nm	0.876	0.77	0.23

Gupta and Seshadriz [10] developed an equation, based on Ouchiyama and Tanaka's model [11]–[13], to calculate the theoretical maximum packing fraction of a polydisperse system of spheres by taking into consideration particle size, size distribution, and modality. The equation is given as follows:

$$\phi_m = \frac{\sum D_i^3 f_i}{\sum (D_i - \bar{D})^3 + \frac{1}{\bar{n}} \sum \left\{ (D_i - \bar{D})^3 - (D_i \sim \bar{D})^3 \right\} f_i} \tag{3}$$

where

$$\bar{n} = 1 + (4/13)\left(8\phi_m^0 - 1\right)\bar{D}\Big(\Big(\sum (D_i + \bar{D})^2 \{1 - (3/8)\left(\bar{D}/D_i + \bar{D}\right)\} f_i\Big) / \Big(\sum \left\{D_i^3 - (D_i - \bar{D})^3\right\} f_i\Big)\Big)$$

and $\bar{D} = \sum D_i f_i$

Here, D_i is the diameter of the ith component, f_i is the number fraction of ith component, and ϕ_m^0 is the maximum packing of spheres of uniform size, and the abbreviation $(D_i - \bar{D})$ is defined as

$$D_i - \bar{D}) = 0 \text{ for } D_i \le \bar{D}$$

and

$$(D_i - \bar{D}) = D_i - \bar{D} \text{ for } D_i \ge \bar{D}.$$

In addition, the number fraction f_i can be calculated from

$$f_i = \frac{\frac{\nu_i}{D_i^3}}{\sum \frac{\nu_i}{D_i^3}}$$

where ν_i is the volume fraction of ith component.

Theoretical maximum packing fractions can be obtained from calculations of the above equations. Table I lists the theoretical maximum packing fraction and the corresponding bimodal filler ratios for each specific system.

Authorized licensed use limited to: IEEE Xplore. Downloaded on October 7, 2008 at 8:41 from IEEE Xplore. Restrictions apply.

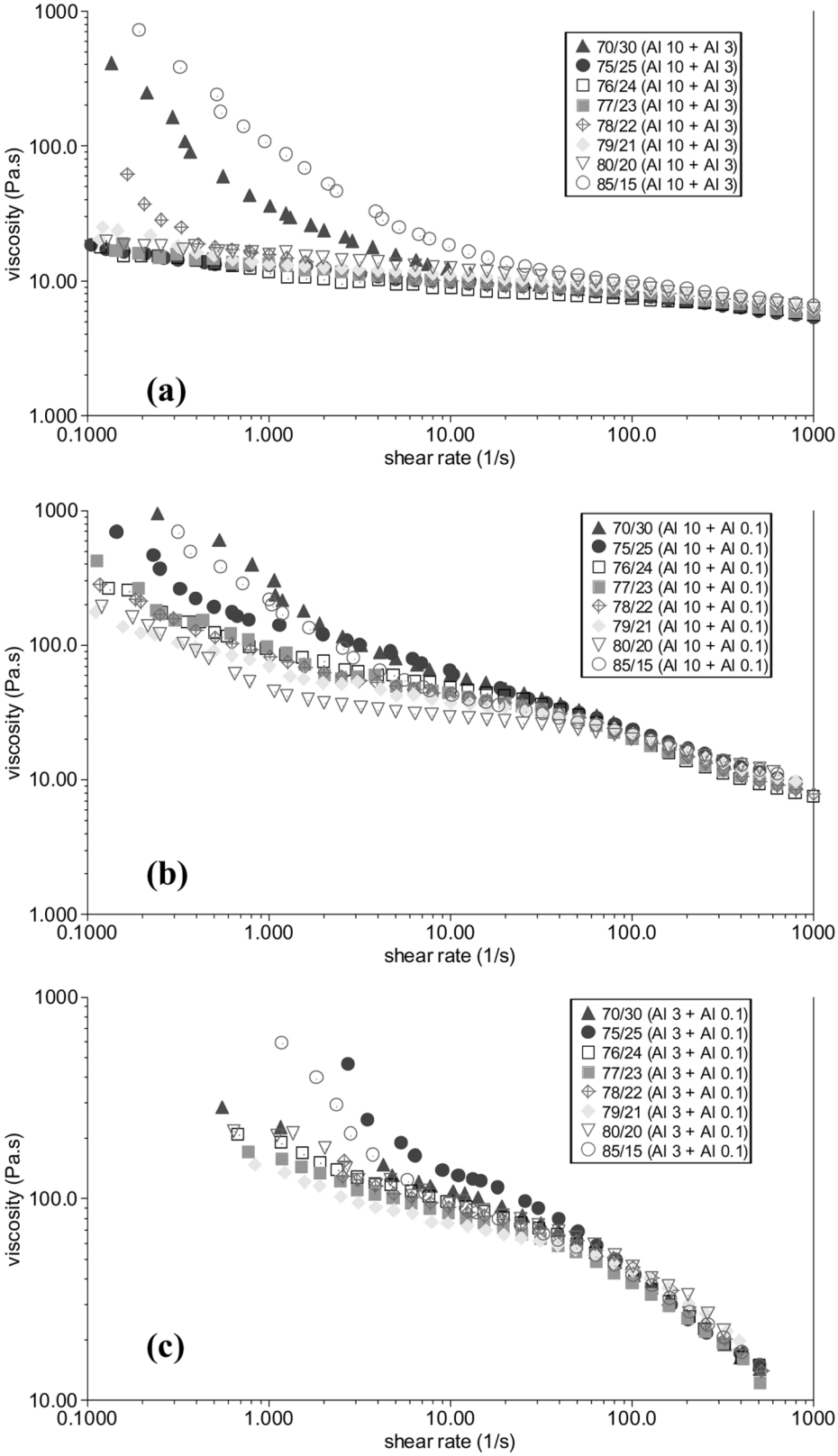

Fig. 15. Shear viscosity as a function of shear rate of bimodal aluminum-filled composites. (a) 10 μm plus 3.0-μm aluminum. (b) 10 μm plus 100-nm aluminum. (c) 3.0 μm plus 100-nm aluminum. In the legend, Al3, Al10, and Al0.1 denote 3.0-μm, 10.0-μm, and 100-nm aluminum, respectively.

According to Table I, 10.0 μm plus 100-nm filler combination has the largest theoretical maximum packing fraction of 0.891, and for all bimodal systems, the maximum packing fractions occur when the volume fraction of large particle to small particle is in the range of 4:1 to 3:1. A set of bimodal filler volume fraction ratios (large particle/small particle), i.e., 70/30, 75/25, 76/24, 77/23, 78/22, 79/21, 80/20, and 85/15 were then chosen to perform rheology studies, in order to find the bimodal filler

Authorized licensed use limited to: IEEE Xplore. Downloaded on October 7, 2008 at 8:41 from IEEE Xplore. Restrictions apply.

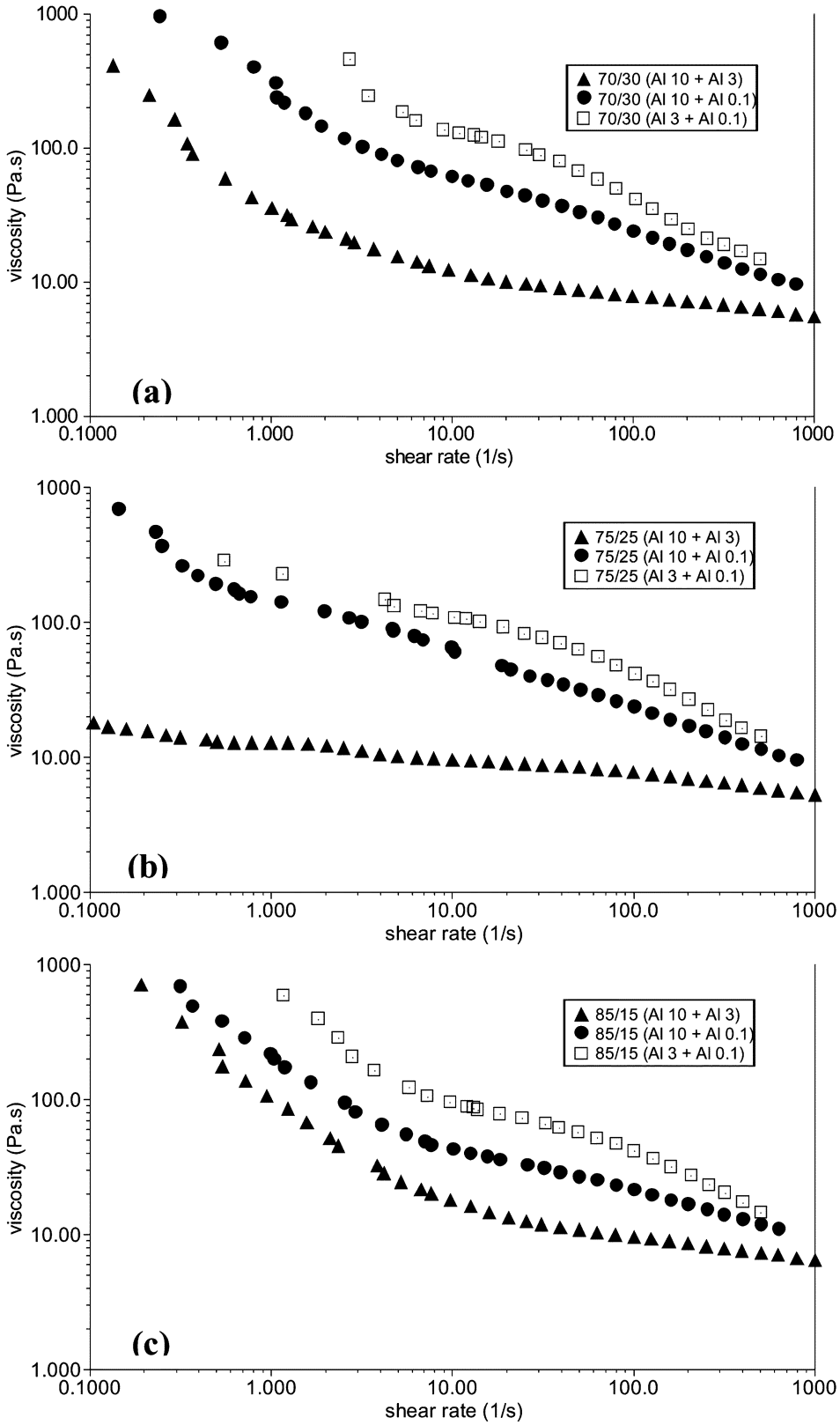

Fig. 16. Comparison of shear viscosity of three bimodal aluminum-filled systems (10.0 μm + 3.0-mum aluminum, 10.0 μm + 100-nm aluminum, and 3.0 μm + 100-nm aluminum) at fixed bimodal filler ratio (a) 70/30, (b) 75/25, and (c) 85/15. In the legend, Al3, Al10, and Al0.1 denote 3.0-μm, 10.0-μm, and 100-nm aluminum, respectively.

volume fraction ratio that gives the minimum viscosity in the bimodal composites when they are filled with the same filler loading level. All composite materials were prepared with the same filler loading of 60 wt%. The experiments were performed under steady-state flow procedure with parallel-plate geometry. Fig. 15 shows plots of shear viscosity as a function of shear rate

Authorized licensed use limited to: IEEE Xplore. Downloaded on October 7, 2008 at 8:41 from IEEE Xplore. Restrictions apply.

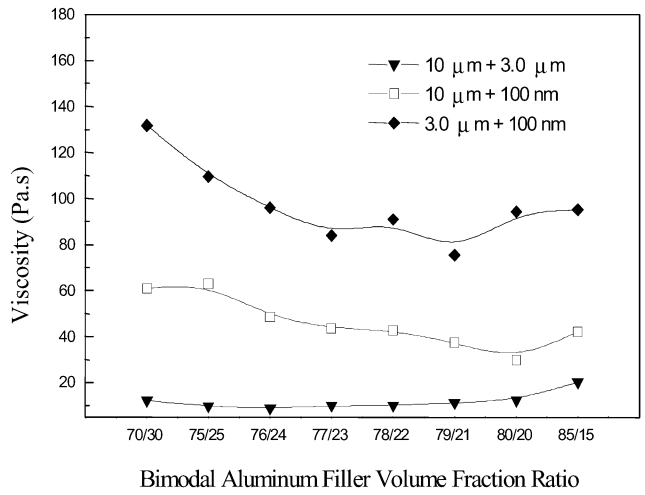

Fig. 17. Viscosity of bimodal aluminum composites as a function of bimodal filler volume fraction ratio at shear rate 10 s^{-1}.

TABLE II
FILLER VOLUME FRACTION RATIOS (LARGE PARTICLE/SMALL PARTICLE) CORRESPONDING TO MINIMUM VISCOSITY OF BIMODAL ALUMINUM-FILLED SYSTEMS

Filler Combination	Bimodal Filler Volume Fraction Ratio at Minimum Viscosity
10 μm + 3.0 μm	76/24
10 μm + 100 nm	80/20
3.0 μm + 100 nm	79/21

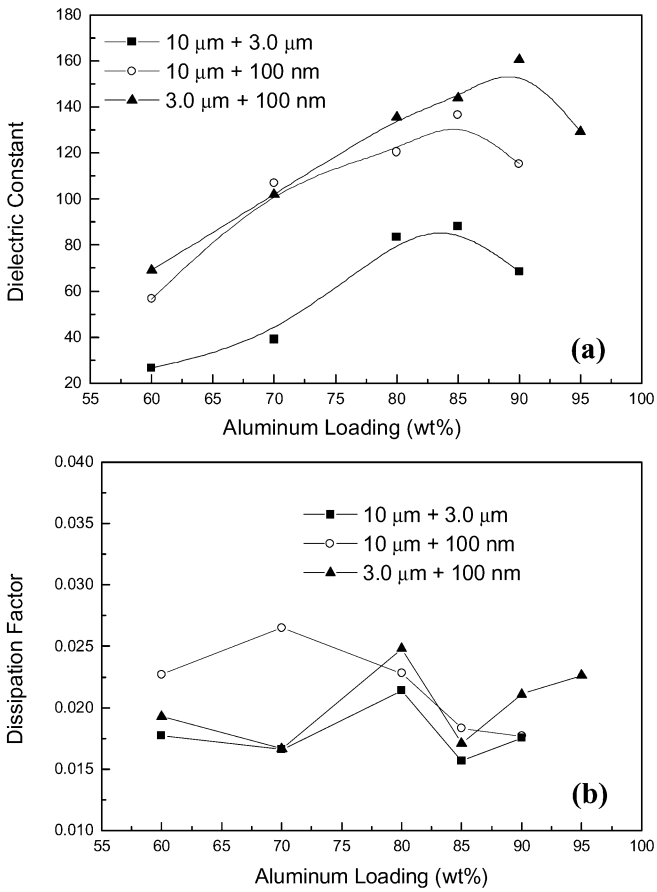

Fig. 18. (a) Dielectric constant and (b) dissipation factor of bimodal aluminum filled composites as a function of aluminum loading level (@ 10 kHz).

of bimodal aluminum filled systems: (a) 10 μm plus 3.0-μm aluminum, (b) 10 μm plus 100-nm aluminum, and (c) 3.0 μm plus 100-nm aluminum. All materials show shear thinning behavior. At a low shear rate, the viscosity of different systems is quite different; however, at high shear rates, the viscosity becomes leveled.

The comparison of shear viscosity of three bimodal aluminum-filled systems (10.0 μm + 3.0-μm aluminum, 10.0 μm + 100-nm aluminum, and 3.0 μm + 100-nm aluminum) at fixed bimodal filler volume fraction ratios (large particle/small particle) is given in Fig. 16. For all bimodal filler ratios, 3.0 μm plus 100-nm aluminum-filled system has the highest viscosity, and 10.0 μm + 3.0- μm aluminum-filled system has the lowest viscosity. Viscosity of filled composites is determined by the volume filler loading level and the interfacial area between filler particles and the epoxy matrix of the composites. Higher filler loading leads to higher viscosity, which makes it more difficult to uniformly disperse the filler in the composites. At fixed filler loading, the viscosity of composites depends on the interfacial area between the filler particles and the epoxy. Because smaller particles overall have larger surface area, which induces more friction during shearing measurement, the combination of smallest bimodal fillers, i.e., 3.0 μm plus 100-nm aluminum, has the highest viscosity.

Fig. 17 shows the viscosity of bimodal aluminum composites at shear rate 10 s^{-1} as a function of bimodal filler volume fraction ratio (large particle/small particle). At the fixed shear rate of 10 s^{-1}, for all three systems, the bimodal filler volume fraction ratio of 70/30 or 85/15 has a higher shear viscosity than other combinations. Minimum shear viscosity is found at bimodal filler volume fraction ratio 76/24 for system with 10.0 μm plus 3.0-μm aluminum, at bimodal ratio 80/20 for system with 10.0 μm plus 100-nm aluminum, and at bimodal ratio 79/21 for system with 3.0 μm plus 100-nm aluminum. The bimodal ratio showing the lowest viscosity at the same filler loading level indicates that such filler combination has the best packing efficiency, and thus the highest filler loading can be obtained at such ratio for the system. These combinations of bimodal filler volume fraction ratio, as listed in Table II, were then selected for further dielectric studies.

Fig. 18(a) shows the dielectric constant and (b) dissipation factor of bimodal aluminum-filled composites at 10 kHz, respectively. The dielectric constant of aluminum-filled composites increases with the filler loading level. With the optimized bimodal filler volume fraction ratio, the highest dielectric constant obtained is 88 for 10.0 μm plus 3.0 μm aluminum-filled system, 136 for 10.0 μm plus 100-nm aluminum-filled system, and 160 for 3.0 μm plus 100-nm aluminum-filled system. Dissipation factors of all composites are around or below 0.025, which is desirable for embedded passive application.

Fig. 19 shows the optical microscope pictures of aluminum-filled composites. (d), (f), and (h) are morphologies of 60 wt% 10.0 μm plus 3.0 μm aluminum-filled composite, 60 wt% 10.0 μm plus 100-nm aluminum-filled composite, and 60 wt% 3.0 μm plus 100-nm aluminum-filled composite, respectively. The fillers at the loading of 60 wt% are not as tightly

Authorized licensed use limited to: IEEE Xplore. Downloaded on October 7, 2008 at 8:41 from IEEE Xplore. Restrictions apply.

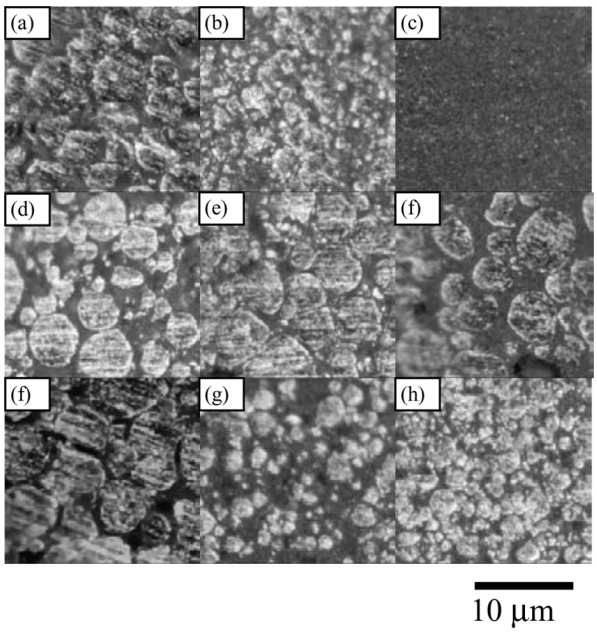

Fig. 19. Optical microscope pictures of aluminum-filled composites. (a) 10.0-μm aluminum at 85 wt. (b) 3.0-μm aluminum at 80 wt%. (c) 100-nm aluminum at 60 wt%. (d) 10.0 μm + 3.0-μm aluminum at 60 wt%. (e) 10.0 μm + 3.0-μm aluminum at 85 wt%. (f) 10.0 μm + 100-nm aluminum at 60 wt%. (g) 10.0 μm + 100-nm aluminum at 85 wt%. (h) 3.0 μm + 100-nm aluminum at 60 wt%. (i) 3.0 μm + 100-nm aluminum at 90 wt%. (a), (b), (c), (e), (g), and (i) are loaded at the filler loading corresponding to the maximum dielectric constant for the filler combination.

packed as those in (e), (g), and (i), which are morphologies of 85 wt% 10.0 μm plus 3.0 μm aluminum-filled composite, 85 wt% 10.0 μm plus 100-nm aluminum-filled composite, and 90 wt% 3.0 μm plus 100-nm aluminum-filled composite, respectively. The tightly packed filler particles at high filler loading in (e), (g), and (i) lead to the maximum dielectric constant of each system. The bimodal composites in (e), (g), and (i) show much higher maximum dielectric constants than unimodal composites in (a) and (b), which is simply due to the higher packing efficiency in the bimodal system. In unimodal composites, only epoxy matrix surrounds the filler particles; however, in bimodal systems, some smaller second filler particles are filled in the gap of bigger major particles.

IV. Conclusion

A novel high dielectric constant composite material was developed by using self-passivation aluminum as the filler. The self-passivated insulating aluminum oxide layer on the aluminum metallic core showed significant effects on the electric and dielectric properties of the corresponding aluminum composites. With the insulating aluminum oxide layer, a high loading level of aluminum can be used while the composite materials continued to be insulating. For composites containing 80 wt% 3.0 μm aluminum, a dielectric constant of 109 and a low dissipation factor of about 0.02 (@10 kHz) were achieved. Aluminum composites had good reliability as shown in the 85/85 aging test, and good adhesion toward copper-laminated substrate as shown in the die shear measurement. Ouchiyama and Tanaka's model was used to calculate the theoretical maximum packing fraction of bimodal system of spheres. Based on this calculation, rheology studies were performed to find the optimum bimodal filler volume fraction ratio that leads to the best packing efficiency of bimodal fillers. It was found that the viscosity of polymer composites showed a minimum at optimum bimodal filler ratio. The minimum shear viscosity occurred at a bimodal filler volume fraction ratio 76/24 for system with 10.0 μm plus 3.0-μm aluminum, at a bimodal filler ratio 80/20 for system with 10.0 μm plus 100-nm aluminum, and at a bimodal filler ratio 79/21 for system with 3.0 μm plus 100-nm aluminum. Such bimodal filler volume fraction ratios can provide the highest filler loading for the specific systems. Using the optimized bimodal filler volume fraction ratio from rheology study, the highest dielectric constant obtained at 10 kHz was 88 for the system filled with 10.0 μm plus 3.0-μm aluminum, 136 for system filled with 10.0 μm plus 100-nm aluminum, and 160 for system filled with 3.0 μm plus100-nm aluminum. The developed aluminum composite is a promising candidate material for embedded capacitor applications.

Acknowledgment

The authors would like to thank Dr. R. Ulrich, Professor in the Department of Chemical Engineering, University of Arkansas, for the helpful discussions on the dielectric behavior and dielectric mechanisms presented in this paper.

References

[1] R. K. Ulrich and L. W. Schaper, *Integrated Passive Component Technology*. New York: Wiley, 2003.
[2] Y. Rao, J. Yue, and C. P. Wong, "High K polymer nano-composite development, characterrization, and modeling for embeddd capacitor RF application," in *Proc. 51st Electron. Compon. Technol. Conf.*, 2001, pp. 1408–1412.
[3] D. M. Grannan, J. C. Garland, and D. B. Tanner, "Critical behavior of the dielectric constant of a random composite near the percolation threshold," *Phys. Rev. Lett.*, vol. 46, no. 5, pp. 375–378, 1981.
[4] D. S. McLachlan, I. I. Oblakova, and A. B. Pakhomov, "The complex dielectric constant of a metal (superconductor)-Insulator system near the percolation threshold," *Phys. B*, vol. 194–196, pp. 2011–2012, 1994.
[5] Y. Song, T. W. Noh, S. Lee, and J. R. Gaines, "Experimental study of the three-dimensional ac conductivity and dielectric constant of a conductor–insulator composite near the percolation threshold," *Phys. Rev. B*, vol. 33, no. 2, pp. 904–908, 1986.
[6] C. Pecharroman and J. S. Moya, "Experimental evidence of a giant capacitance in insulator–conductor composites at the percolation threshold," *Adv. Mater.*, vol. 12, no. 4, pp. 294–297, 2000.
[7] Y. Rao, C. P. Wong, and J. Xu, "High Dielectric Polymer Composites and Methods of Preparation Thereof," U.S. Patent 6 864 306, Apr. 30, 2002.
[8] N. F. Mott, "Oxidation of metals and the formation of protective films," *Nature*, vol. 145, pp. 996–996, 1940.
[9] A. J. Poslinski, M. E. Ryan, R. K. Gupta, S. G. Seshadri, and F. J. Frechette, "Rheological behavior of filled polymeric systems II. The effect of a bimodal size distribution of particulates," *J. Rheol.*, vol. 32(B), pp. 751–771, 1988.
[10] R. K. Gupta and S. G. Seshadri, "Maximum loading levels in filled liquid systems," *J. Rheol.*, vol. 30, no. 3, pp. 503–508, 1986.
[11] N. Ouchiyama and T. Tanaka, "Estimation of the average number of contacts between randomly mixed solid particles," *Ind. Eng. Chem. Fund.*, vol. 19, pp. 338–340, 1980.
[12] ——, "Porosity of a mass of solid particles having a range of sizes," *Ind. Eng. Chem. Fund.*, vol. 20, pp. 66–71, 1981.
[13] ——, "Porosity estimation for random packings of spherical particles," *Ind. Eng. Chem. Fund.*, vol. 23, pp. 490–493, 1984.

Authorized licensed use limited to: IEEE Xplore. Downloaded on October 7, 2008 at 8:41 from IEEE Xplore. Restrictions apply.

Jianwen Xu (M'05) received the B.S. degree from Shanghai Jiaotong University, Shanghai, China, in 1995 and the M.S. degree from the Zhejiang University, Hangzhou, China in 2001. He is currently pursuing the Ph.D. degree at the School of Materials Science and Engineering, Georgia Institute of Technology, Atlanta.

Kyoung-Sik Moon, photograph and biography not available at the time of publication.

Christopher Tison, photograph and biography not available at the time of publication.

C. P. Wong (F'92) received the B.S. degree in chemistry from Purdue University, West Lafayette, IN, and the Ph.D. degree in chemistry from Pennsylvania State University, University Park, in 1975.

After his doctoral study, he was awarded two years as a Postdoctoral Scholar at Stanford University, Stanford, CA, with Prof. Henry Taube. He joined AT&T Bell Laboratories, PA, in 1977 as Member of Technical Staff. He was elected an AT&T Bell Laboratories Fellow in 1992. He is a Regents Professor with the School of Materials Science and Engineering and a Research Director at the National Science Foundation (NSF)-funded Packaging Research Center, Georgia Institute of Technology (Georgia Tech), Atlanta. He holds over 40 U.S. patents, numerous international patents, and has published over 400 technical papers and 400 keynotes and presentations in related areas. His research interests lie in the fields of polymeric materials, high-Tc ceramics, materials reaction mechanism, IC encapsulation, in particular, hermetic equivalent plastic packaging, electronic manufacturing packaging processes, flip-chip underfill materials, high K, high-Q embedded passives, interfacial adhesions, PWB, SMT assembly, and components reliability.

Dr. Wong received the AT&T Bell Laboratories Distinguished Technical Staff Award in 1987, the AT&T Bell Fellow Award in 1992, the IEEE Components, Packaging and Manufacturing Technology (CPMT) Society Outstanding and Best Paper Awards in 1990, 1991, 1994, 1996, 1998, and 2002, the IEEE Technical Activities Board Distinguished Award in 1994, the 1995 IEEE CPMT Society's Outstanding Sustained Technical Contribution Award, the 1999 Georgia Tech Outstanding Faculty Research Program Development Award, the 1999 NSF-Packaging Research Center Faculty of the Year Award, the 1999 Georgia Tech Sigma Xi Faculty Best Research Paper Award, the University Press (London, U.K.) Award of Excellence, and was elected a member of the National Academy of Engineering in 2000. He served as the Technical Vice President (1990 and 1991), and President (1992 and 1993) of the IEEE CPMT Society.

Authorized licensed use limited to: IEEE Xplore. Downloaded on October 7, 2008 at 8:41 from IEEE Xplore. Restrictions apply.